

Acid-free Hydrothermal Process for Synthesis of Bioactive Glasses $70\text{SiO}_2-(30-x)\text{CaO}-x\text{ZnO}$ ($x = 1, 3, 5 \text{ mol.}\%$)[†]

Ta Anh Tuan¹, Elena V. Guseva¹, Le Hong Phuc², Nguyen Quan Hien², Nguyen Viet Long³ and Bui Xuan Vuong^{4,*}

¹ Faculty of Chemical Technologies, Kazan National Research Technological University, Marksa 68, 420015 Kazan, Russia; taanhtuan84pt@hpu2.edu.vn (T.A.T.); leylaha@mail.ru (E.V.G.)

² Ho Chi Minh City Institute of Physics, Vietnam Academy of Science and Technology, 01 Mac Dinh Chi St, District 01, Ho Chi Minh City 700000, Vietnam; lhphuc@hcmip.vast.vn (L.H.P.); quanhiengv@yahoo.com.vn (N.Q.H.)

³ Department of Electronics and Telecommunication, Sai Gon University, Ho Chi Minh City 700000, Vietnam; nguyenviet_long@yahoo.com

⁴ Faculty of Pedagogy in Natural Sciences, Sai Gon University, Ho Chi Minh City 700000, Vietnam

* Correspondence: buixuanvuongsgu@gmail.com; Tel.: +84-02838354409

† Presented at the 2nd International Electronic Conference on Crystals, 10–20 November 2020; Available online: https://iocc_2020.sciforum.net/.

Published: 31 December 2020

Abstract: Bioactive glasses $70\text{SiO}_2-(30-x)\text{CaO}-x\text{ZnO}$ ($x = 1, 3, 5 \text{ mol.}\%$) were prepared by the acid-free hydrothermal method in keeping with green chemical technology. The synthetic glasses were investigated by TG-DSC, BET, XRD, and SEM-EDX methods. All synthetic glasses present mesoporous structures consisting of aggregates of nanoparticles. The bioactivity of synthetic glasses was confirmed through the formation of the hydroxyapatite phase after an in vitro experiment in simulated body fluid (SBF) solution. The effect of Zn addition is shown through the decrease in the bioactivity of synthetic glasses. Additionally, the inductively coupled plasma optical emission spectrometry (ICP-OES) analysis indicates that the Zn ions were released from the glassy networks during in vitro experiments, and they act as $\text{Zn}(\text{OH})_2$ suspended precipitation to inhibit the apatite deposition. The in vitro experiment in cell culture matter was performed for SaOS₂ and Eahy929 cells. The results confirm the biocompatibility of synthetic glasses and the role of Zn addition in the proliferation of living cells.

Keywords: bioactive glasses; bioactivity; sol–gel; hydrothermal; in vitro experiment

1. Introduction

For the past five decades, bioactive glasses have been used as artificial bone materials thanks to their typical ability to connect to the natural bone by forming a hydroxyapatite layer during in vitro and in vivo experiments [1]. These biomaterials can be synthesized by using two main methods: melting and sol–gel [2]. Recently, the sol–gel method has been widely applied because it has more advantages than the melting method. This method can produce bioactive glasses at moderate temperatures, preventing the final product loss because of P_2O_5 evaporation. Furthermore, this method is able to synthesize bioactive glasses at with mesoporous structures and high values of specific surface area, which reinforces the bioactivity of obtained materials [3,4]. To control the bioactivity and biocompatibility of sol–gel glasses, beneficial elements such as Mg, Sr, Al, Cu, Fe, Ag, and Zn have been added [5–11]. Among them, Zn plays an important role in bone formation because of its ability to inhibit the activity of osteoclasts and increase the differentiation of osteoblasts [12,13].

Depending on the content of the doped Zn as well as the composition of the system, the synthetic glass systems exhibit different properties. Bioactive glass $64\text{SiO}_2\text{-}26\text{CaO-}5\text{P}_2\text{O}_5\text{-}5\text{ZnO}$ (mol.%) has been elaborated by A. Balamurugan et al. using the sol-gel method. The authors pointed out that the incorporation of ZnO not only reduces the bioactivity of synthetic glass but also increases the osteoblast proliferation [6]. Abeer M. El-Kady et al. have fabricated various sol-gel glasses $58\text{SiO}_2\text{-}(33\text{-}x)\text{CaO-}9\text{P}_2\text{O}_5\text{-}x\text{ZnO}$ ($x = 1, 3, 5$ wt.%) [14]. All synthetic glasses exhibited high porosities, surface areas, and good bioactivity in the simulated body fluid (SBF) test. Ternary $60\text{SiO}_2\text{-}36\text{CaO-}4\text{P}_2\text{O}_5$ (mol.%) and quaternary $60\text{SiO}_2\text{-}25\text{CaO-}11\text{Na}_2\text{O-}4\text{P}_2\text{O}_5$ (mol.%) sol-gel glasses doped with 0, 1, 5 and 10 mol.% of ZnO have been synthesized by Julian Bejarano [15]. The study indicated the content of doped ZnO influenced the textures, bioactivity, and compatibility of synthetic glasses. Furthermore, the increase in doped ZnO caused the decrease in the formation of apatite mineral on the surface of the glass after in vitro experiments. Thus, many glass systems containing ZnO have been studied by the sol-gel method. However, most synthesized ZnO-containing glasses used harmful strong acids and bases as catalysts for the hydrolysis process. In our previous study, the acid-free hydrothermal method was used for synthesized binary bioactive glass with the molar composition of 70%SiO₂-30%CaO [16]. A combination of starting precursors without acid catalysts was heat-treated in a hydrothermal reactor at 150 °C for 24 h. The obtained product in concentrated gel was dried and sintered at 700 °C for 3 h. The synthetic glass was an amorphous structure and presented interesting bioactivity. Based on this approach, we synthesize the ternary bioactive glasses $70\text{SiO}_2\text{-}(30\text{-}x)\text{CaO-}x\text{ZnO}$ (mol.%, $x = 1, 3, \text{ and } 5$) within the present work.

The effects of ZnO additions on the physical-chemical properties, bioactivities, and biocompatibilities of synthetic bioactive glasses were investigated.

2. Materials and Methods

2.1. Acid-Free Synthesis of Bioactive Glasses Containing ZnO

New series of bioactive glasses $70\text{SiO}_2\text{-}(30\text{-}x)\text{CaO-}x\text{ZnO}$ (mol.%, $x = 1, 3, 5$) were synthesized by the hydrothermal method according to the previous study [16]. Briefly, a mixture of tetraethyl orthosilicate (TEOS, Merck, 99.0%), $\text{Ca}(\text{NO}_3)_2 \cdot 4\text{H}_2\text{O}$ (Merck, 100%), $\text{Zn}(\text{NO}_3)_2 \cdot 6\text{H}_2\text{O}$ (Merck, 98%), and H_2O was put into a hydrothermal system consisting of a stainless-steel autoclave with a Teflon core. The reactive system was performed at 150 °C for 1 day. The obtained gel was dried at 150 °C to make the ceramic powders. The bioactive glasses were achieved by sintering the powders at 700 °C for 3 h. We denoted the bioactive glasses $70\text{SiO}_2\text{-}(30\text{-}x)\text{CaO-}x\text{ZnO}$ with $x = 1, 3, \text{ and } 5$ mol.% of ZnO as bioglass-Z1, bioglass-Z3, and bioglass-Z5, respectively.

2.2. In Vitro Test in SBF Solution

The bio-mineralization was verified by the immersion of bioactive glasses in the simulated body fluid (SBF) according to the method of Kokubo [17]. The SBF synthetic solution has an inorganic ion concentration similar to that of human blood. Glass powder samples with a mass of 125 mg were soaked in 250 mL of SBF at 37 °C with a stirring rate of 120 rpm for 1, 3, 5, and 7 days. At the end of each immersion phase, the powder samples were refined, dried, and used to determine their physical-chemical characterizations. The remaining solutions are served to measure the ionic concentration.

2.3. In Vitro Test with Cell Culture

Two cell lines SaOS₂ and Eahy929 were selected for culturing in Dulbecco's modified Eagle's medium (DMEM, Merck, Singapore) at 37 °C in a humid environment (95% humidity, 5% CO₂) for 24 h. The test ratio of glass sample/medium was chosen as 0.1 g/mL consistent with the ISO standard 10993-12:2007. The cell viabilities were determined by the MTT method following the previous report [18].

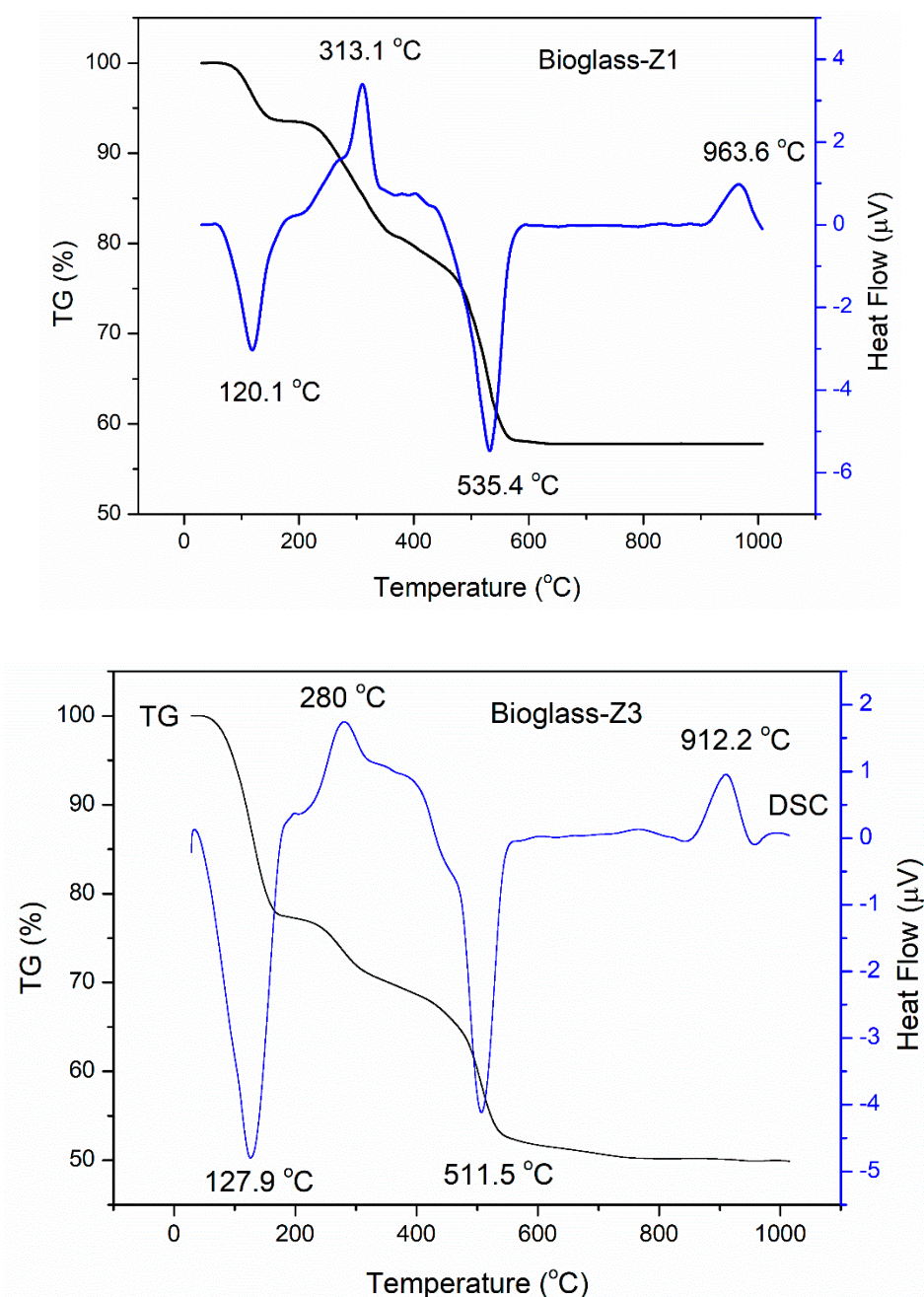
2.4. Physical-Chemical Characterization

The thermal analysis was performed by employing thermogravimetry–differential scanning calorimetry (TG-DSC, Labsys Evo Setaram). X-ray diffraction (XRD, D8-Advance) was served for phase identification. The values of specific surface area, pore size, and pore volume were examined by N₂ adsorption/desorption method (Method BET: Brunauer – Emmett – Teller) (Quantachrome Instruments). The morphology and elemental composition were investigated by using scanning electron microscopy (SEM) associated with energy dispersive X-ray spectroscopy (EDX) (SEM, S-4800, Japan). The ion behavior in SBF fluid was monitored by using inductively coupled plasma optical emission spectrometry (ICP-OES, ICP 2060).

3. Results and Discussion

3.1. Thermal Behavior

Figure 1 presents the TG-DSC curves of bioglass-Z1, bioglass-Z3, and bioglass-Z5.



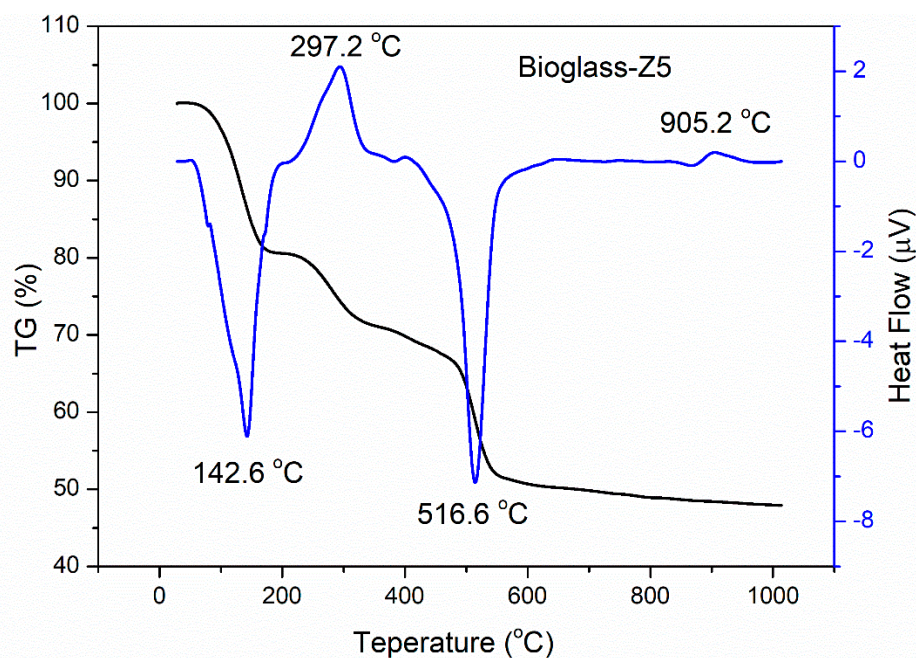


Figure 1. Thermogravimetry–differential scanning calorimetry (TG-DSC) curves of bioactive glasses $70\text{SiO}_2-(30-x)\text{CaO}-x\text{ZnO}$ (mol.%, $x = 1, 3, 5$).

All glasses exhibited three mass-losses within the temperature ranges of 30–200, 200–400, and 400–600 °C. The primary mass-loss is characteristic for the removal of physically adsorbed water. This is shown on the DSC curves of bioglass-Z1, bioglass-Z3, and bioglass-Z5 as the first endothermic peaks centered at 120.1, 127.9, and 142.6 °C, respectively [19]. The second mass-loss with exothermic peaks concentrated at 313.1, 280, and 297.2 °C on the DSC curves of bioglass-Z1, bioglass-Z3, and bioglass-Z5, respectively, is due to the discharge of chemically adsorbed water [20]. The third mass-loss with endothermic peaks centered at 535.4, 511.5, and 516.6 °C on the DSC curves of bioglass-Z1, bioglass-Z3, and bioglass-Z5, respectively, is related to the decomposition of nitrate groups [21]. An exothermic peak without mass-loss at 963.6, 912.2, and 905.2 °C was observed on the DSC curves for bioglass-Z1, bioglass-Z3, and bioglass-Z5, respectively. This corresponds to the phase transition of the glass [21]. The obtained result shows that the phase transition temperature decreased as the ZnO content in the glass increased. This demonstrates the effect of ZnO addition on the thermal properties of synthetic glasses as observed in the previous study [14]. From the thermal analysis, the sintering temperature for synthesis of bioactive glasses was selected as 700 °C.

3.2. Phase Analysis

XRD patterns of synthetic glasses bioglass-Z1, bioglass-Z3, and bioglass-Z5 are presented in Figure 2. The obtained result indicated the amorphous nature of all synthetic glasses, no crystalline peaks were observed. As observed, the center of the diffraction halo was shifted to the right as the ZnO content increased from 1 to 5 mol.%. According to previous studies, Zn acts as Si to form the glassy network and can also replace Ca to act as a network modifier [14,22]. Therefore, this phenomenon can be explained by the successful introduction of Zn^{2+} ions intertwined in the glass networks.

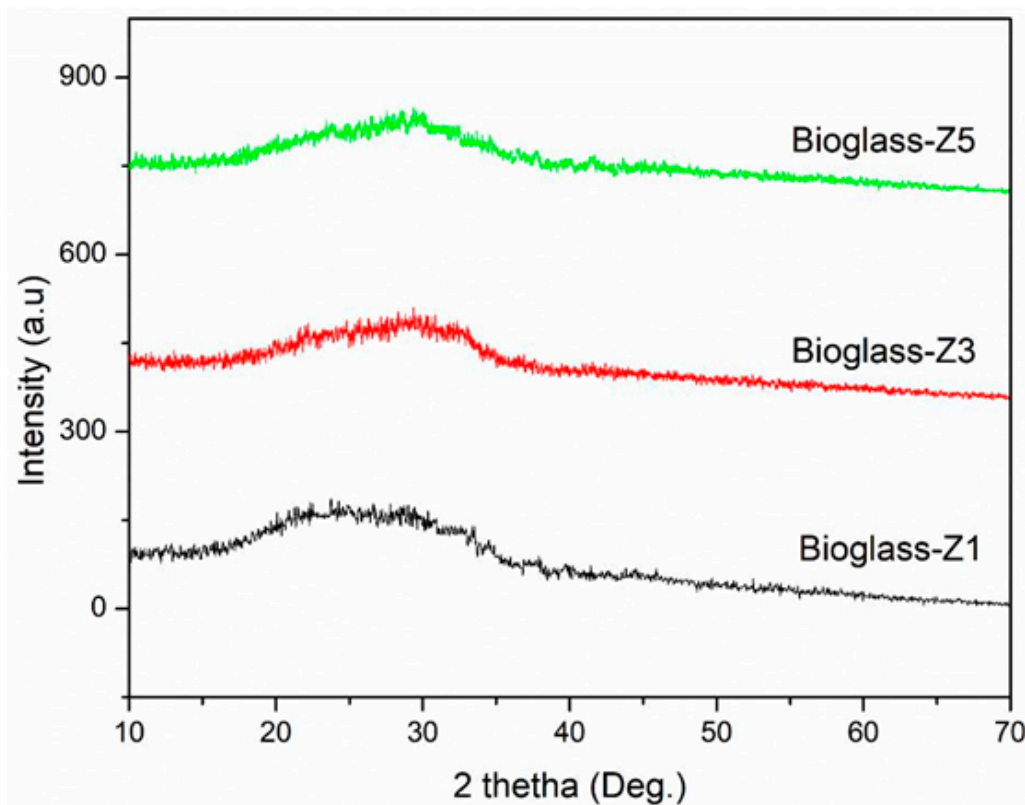


Figure 2. XRD patterns of bioactive glasses $70\text{SiO}_2-(30-x)\text{CaO}-x\text{ZnO}$ (mol.%, $x = 1, 3, 5$).

3.3. Textural Characterization

From the nitrogen adsorption/desorption measurement, the mesoporous properties of synthetic bioactive glasses were obtained, as shown in Table 1. The obtained result indicates that the ZnO addition induced the reduction in porous structures of synthetic bioactive glasses. This is in line with previous research studies, where the authors have shown that the incorporation of divalent ions such as Mg, Cu, Sr, or Zn significantly reduced the porous properties of synthetic glasses [23,24]. The presence of Zn ions may disrupt the orderly association of the SiO_4 tetrahedra within the self-assembly reaction, resulting in structural defects of the silica network, leading to the changes in the mesoporous structures of synthetic bioactive glasses.

Table 1. Values of specific surface area, pore diameter, and pore volume for synthetic glasses.

Samples	Specific Surface Area (m ² /g)	Pore Diameter (nm)	Pore Volume (cm ³ /g)
Bioglass-Z1	133.6	20.8	0.78
Bioglass-Z3	109.5	18.4	0.51
Bioglass-Z5	74.9	18.2	0.34

Figure 3 represents the SEM–EDX analyses of synthetic bioactive glasses. Observing the SEM images shows that bioglass-Z1 exhibited a rough and porous surface while bioglass-Z3, and bioglass-Z5 had less porous surfaces. This observation is consistent with the above result obtained from the nitrogen adsorption/desorption analysis, confirming the effect of ZnO addition on the porous structure reduction in synthetic glasses. The EDX analyses confirmed the presence of the Zn element on the structure of synthetic bioactive glasses.

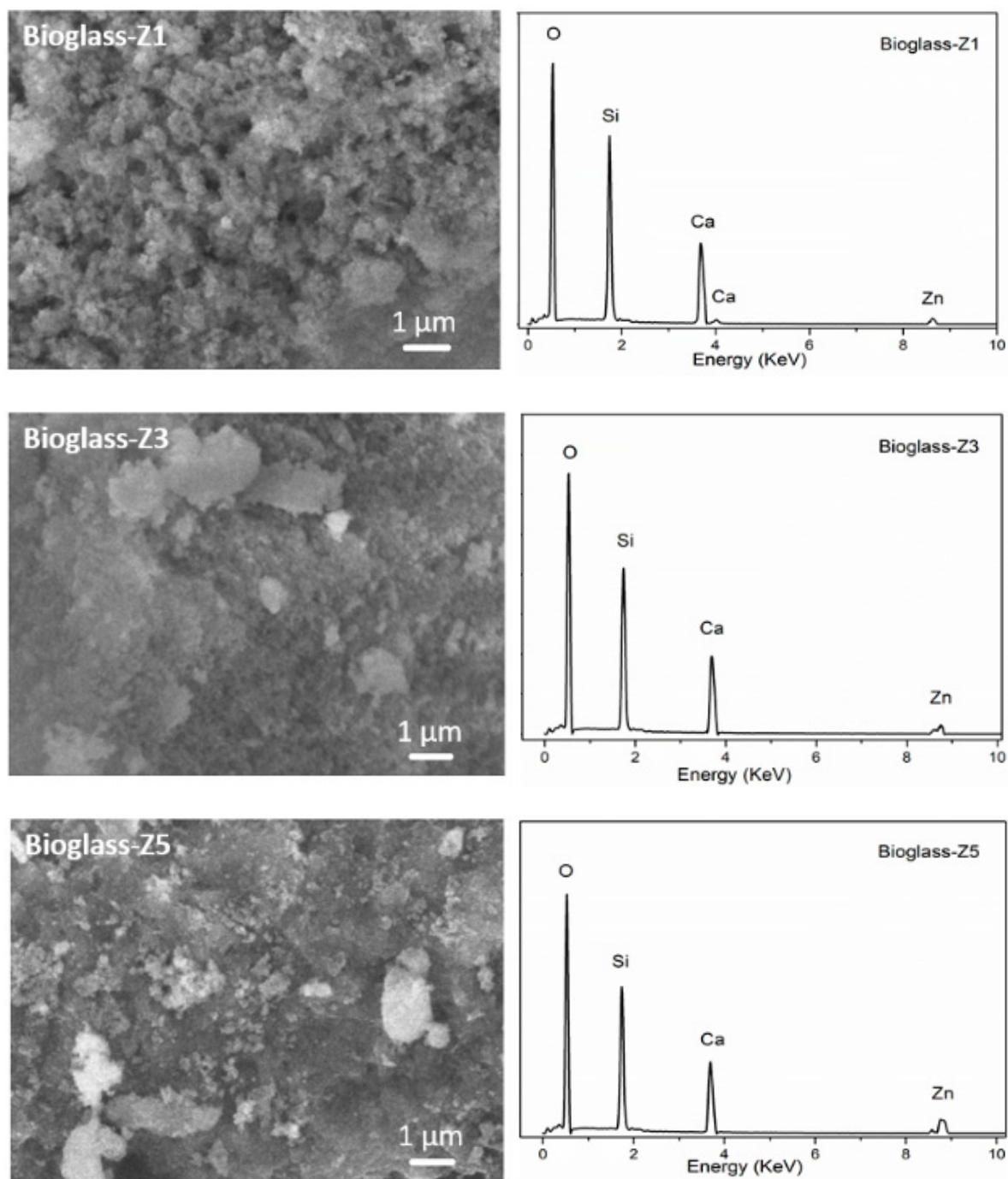


Figure 3. SEM–EDX analyses of bioactive glasses $70\text{SiO}_2-(30-x)\text{CaO}-x\text{ZnO}$ (mol.%, $x = 1, 3, 5$).

3.4. Bio-Mineralization

Figure 4 shows the XRD diagrams of bioactive glasses after 5 days of immersion within the SBF solution. Two well-defined peaks at about $2\theta = 26^\circ$ (002) and 32° (211) were observed for all glass samples. These characteristic peaks are contributed to the crystalline hydroxyapatite (HA) phase (JCPDS file no. 90432). This confirmed the bioactivity of all synthetic glasses. As the ZnO contents increased, two characteristic peaks of HA showed less sharpness and lower intensity. The bioactivity of synthetic glasses can be arranged as bioglass-Z1 > bioglass-Z3 > bioglass-Z5. This phenomenon is in line with the result achieved in previous research studies, confirming the effect of ZnO addition on the bioactivity of synthetic glasses [23,24].

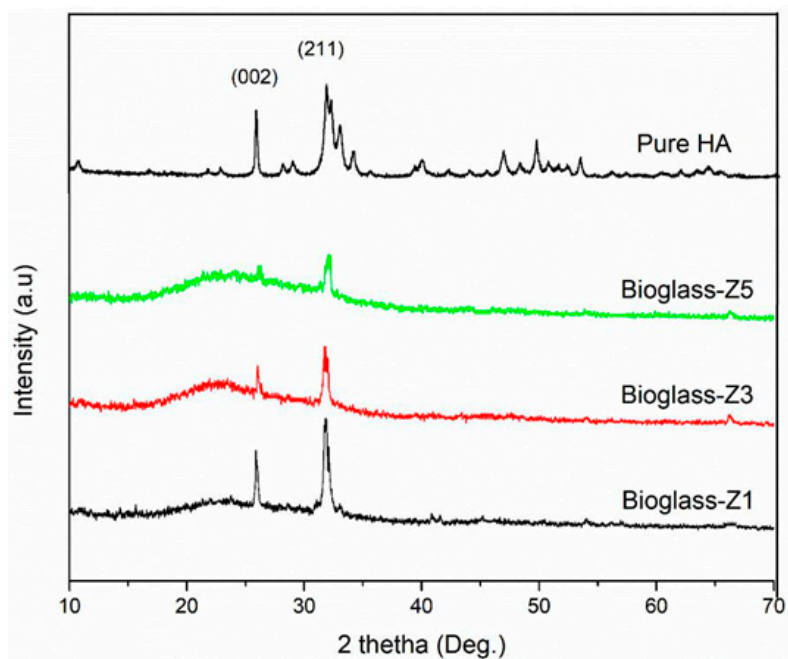
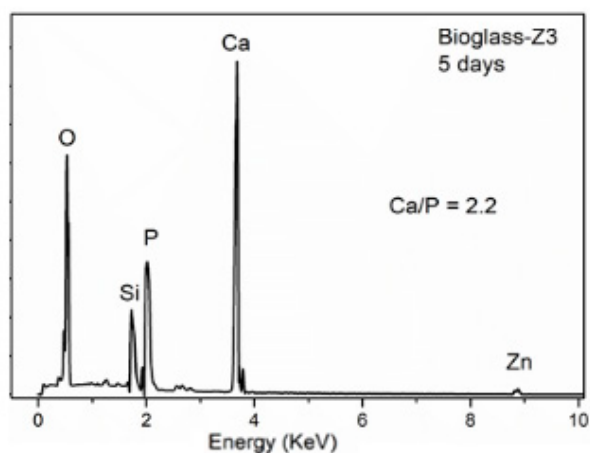
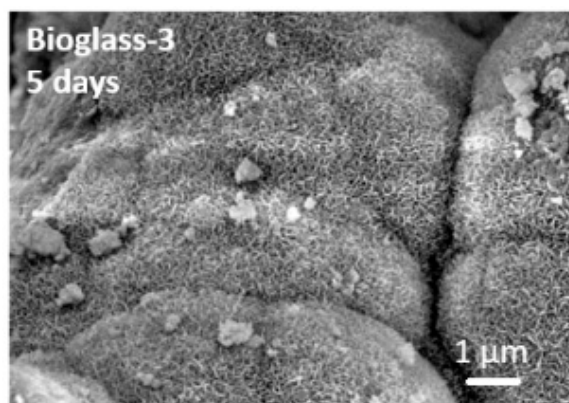
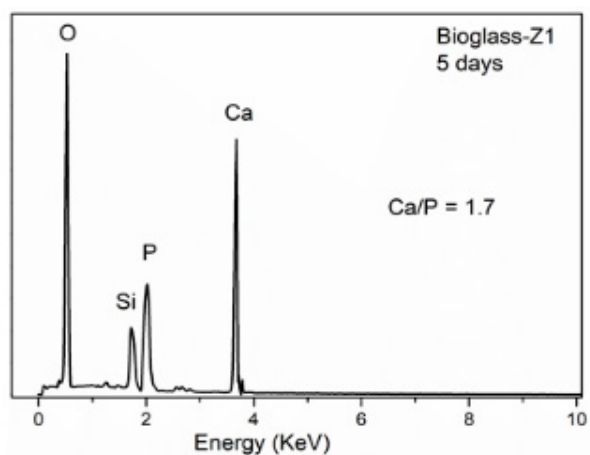
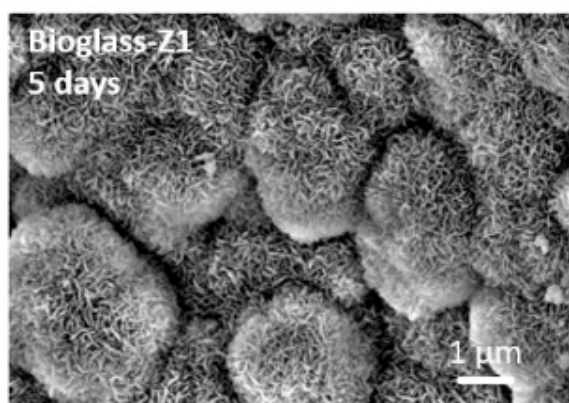


Figure 4. XRD diagrams of bioactive glasses $70\text{SiO}_2-(30-x)\text{CaO}-x\text{ZnO}$ (mol.%, $x = 1, 3, 5$).



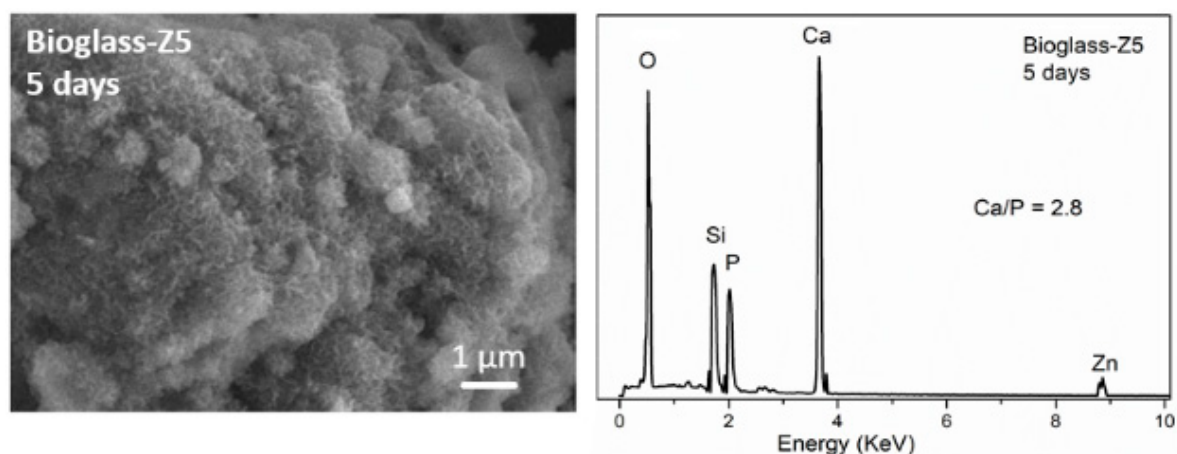
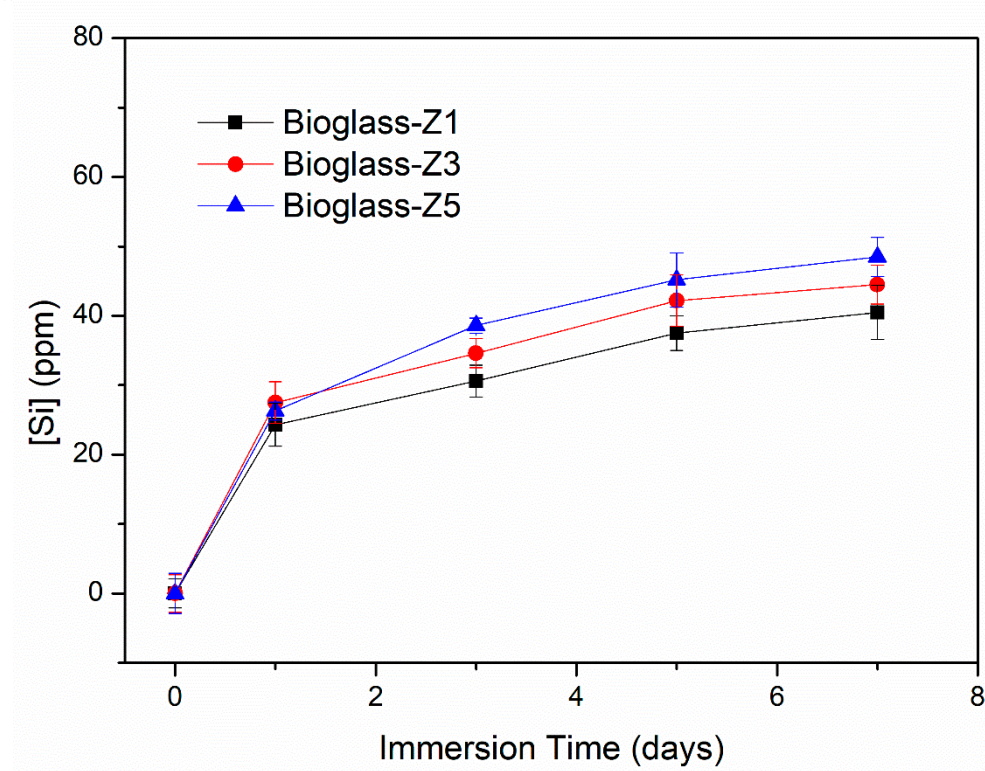
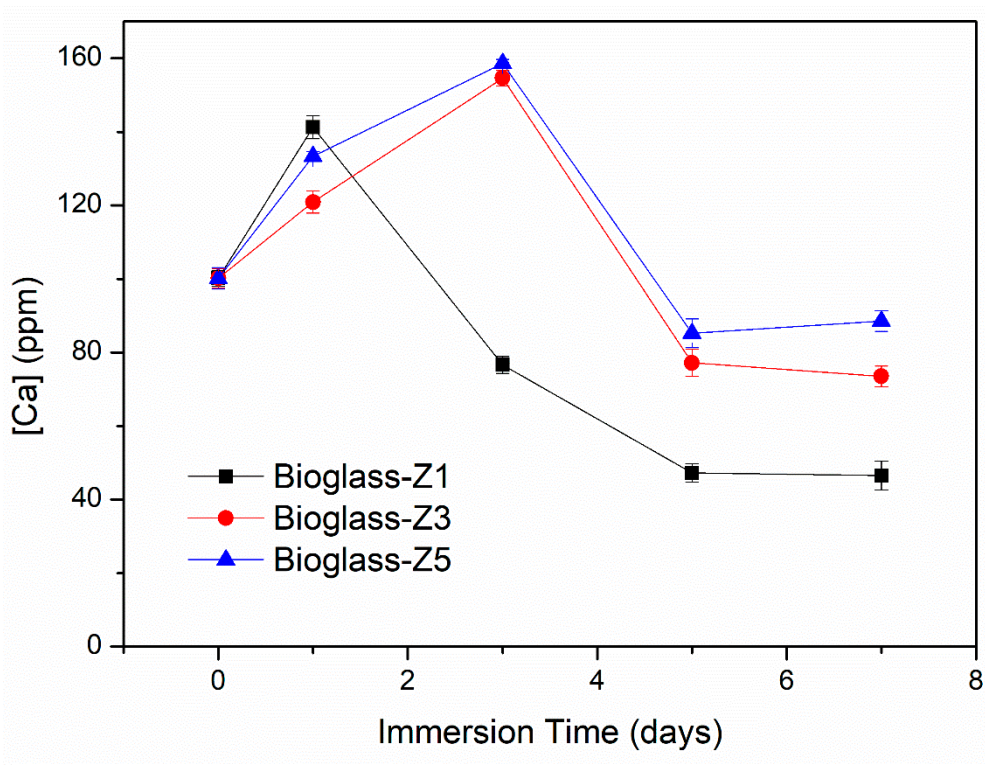


Figure 5. SEM–EDX analyses of bioactive glasses $70\text{SiO}_2-(30-x)\text{CaO}-x\text{ZnO}$ (mol.%, $x = 1, 3, 5$) after 5 days in simulated body fluid (SBF) solution.

The SEM micrographs including EDX analyses of bioactive glasses after 5 days of immersion within the SBF solution are shown in Figure 5. The surfaces of all bioactive glasses were roofed by uniform, dense crystal layers. From the XRD analyses, this observation confirmed the hydroxyapatite formation on the surfaces of bioactive glasses after the in vitro experiment. The HA layer on the surface of bioglass-Z1 is more clearly defined than that of bioglass-Z3, and bioglass-Z5. The EDX analysis of glass samples after 5 days of soaking in the SBF solution showed a sharp decrease in Si content because of the dissolution of the glass network. Meanwhile, Ca and P contents of soaked samples clearly increased, confirming the precipitation of Ca^{2+} and PO_4^{3-} ions to create the apatite layer on the surface of bioactive glasses. The molar Ca/P ratios for the samples bioglass-Z1, bioglass-Z3, and bioglass-Z5 are 1.7, 2.2, and 2.8, respectively. The molar Ca/P ratio of hydroxyapatite (HA) is 1.67. Therefore, sample bioglass-Z1 showed the best forming ability of the HA layer compared to samples bioglass-Z3 and bioglass-Z5.

Ionic changes within the SBF solution are associated with the physical-chemical reactions between the Zn-containing bioactive glasses and the physiological medium (Figure 6). The initial SBF fluid contains 100 ppm of Ca, 0 ppm of Si, 31 ppm of P, and 0 ppm of Zn. After the in vitro experiment, the ionic-exchange behaviors are quite similar for all bioactive glasses. The Ca concentration increased and then decreased. The Si and Zn concentrations increased gradually while the P concentration decreased. The increase in Ca concentration is due to the rapid exchange between the Ca^{2+} ions of the glassy network and H^+ ions in the physiological fluid [1]. Subsequently, the Ca concentration plummeted to achieve saturation at 5 days of immersion. The decrease in Ca concentration is expounded to its consumption to form the mineral HA on the surface of bioactive glasses [1,2]. As well as the decrease in Ca concentration, the P concentration was noted to decrease because of its consumption to form the apatite mineral layer [1,2]. It can be seen that the consumption of Ca and P to form the HA layer of bioglass-Z1 is the most, followed by bioglass-Z3, and bioglass-Z3. The Si concentration increased rapidly on the first day of soaking, then moderately increased to succeed in saturation at 5 days. The increase in Si concentration is explained by the solubility of the glassy network through the discharge of $\text{Si}(\text{OH})_4$ acids while the saturation process corresponds to the self-assembly reactions of the above acids to form the silica SiO_2 layer [1–3]. The amount of Zn released increased in the order bioglass-Z1, bioglass-Z3, and bioglass-Z5, in keeping with the content of ZnO added to the synthetic glasses. According to the literature [23,26], a component of the Zn ions released will form the $\text{Zn}(\text{OH})_2$ precipitation, which prevents the deposition of HA on the glass surfaces. This is suitable when the precipitation of HA decreases as the concentration of added ZnO increases in synthetic glasses.



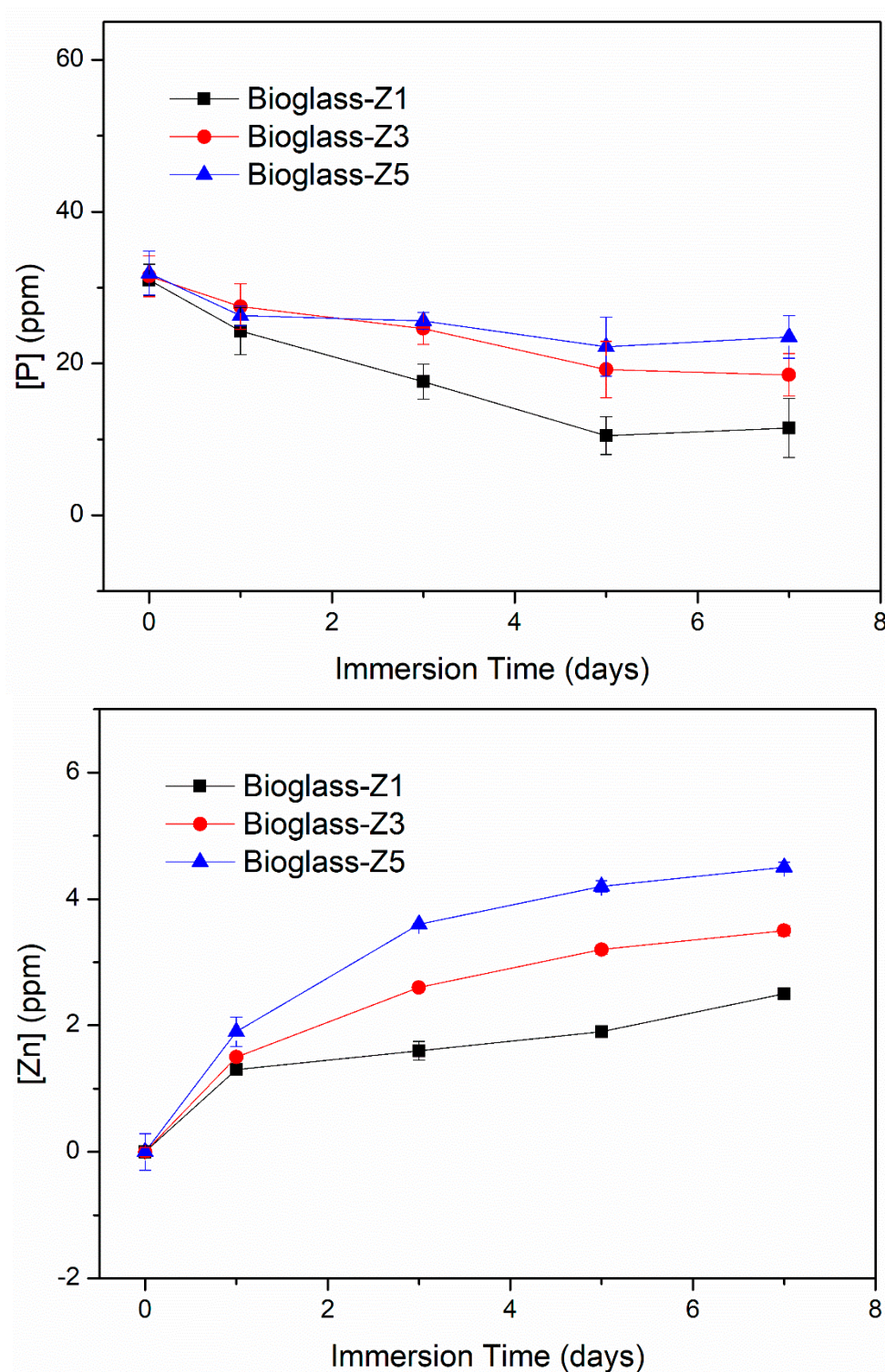


Figure 6. Ionic exchange between bioactive glasses $70\text{SiO}_2-(30-x)\text{CaO}-x\text{ZnO}$ (mol.%, $x = 1, 3, 5$) and SBF solution.

3.5. Biocompatibility

Figure 7 shows the cell viability of the SaOS₂ and Eahy929 lines when exposed to the bioactive glasses for 24 h. Cell viability without glass contact was chosen as the control (100%) [18]. According to the ISO standard 10993-5 (in vitro test for cytotoxicity), cell viability is set as a percentage relative to the control. If the cell viability is a smaller amount than 70%, the material is cytotoxic. Therefore, all synthetic bioactive glasses (bioglass-Z1, bioglass-Z3, and bioglass-Z5) have good biocompatibility. The bioglass-Z5 exhibits the foremost effective biocompatibility compared with the samples bioglass-

Z3, and bioglass-Z1. The obtained results are consistent with previous studies, confirming the effect of ZnO addition on the enhancement of cell viabilities [14,15].

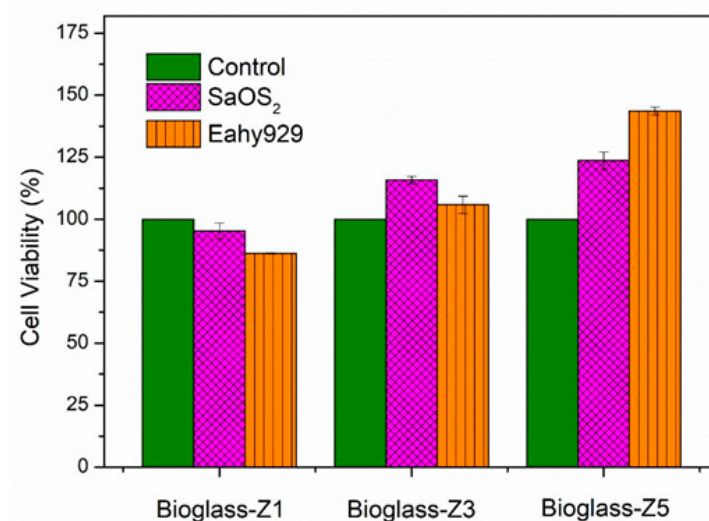


Figure 7. Cell viabilities on bioactive glasses $70\text{SiO}_2-(30-x)\text{CaO}-x\text{ZnO}$ (mol.%, $x = 1, 3, 5$) for 24 h.

4. Conclusions

The study confirmed that the acid-free hydrothermal process was suitable for the synthesis of the bioactive glasses $70\text{SiO}_2-(30-x)\text{CaO}-x\text{ZnO}$ (mol.%, $x = 1, 3, 5$). All synthetic glasses have an amorphous nature. The bioactivity of synthetic glasses was confirmed by the formation of a new layer of hydroxyapatite mineral on the surface of the glass samples after the in vitro test in SBF liquid. The effectiveness of the ZnO addition was shown by inhibiting the bioactivity of synthetic glasses. The in vitro test within the cellular medium confirmed the good biocompatibility of the synthetic glasses and also the positive effect of ZnO addition on cell viability.

Author Contributions: T.A.T.: methodology, experimental, analysis; E.V.G.: methodology, writing, editing; B.X.V.: writing, analysis, editing. All authors have read and agreed to the published version of the manuscript.

Conflicts of Interest: The authors declare no conflict of interest

Reference

1. Hench, L.L. The story of Bioglass. *J. Mater. Sci. Mater. Med.* **2006**, *17*, 967–978.
2. Jones, J.R. Review of bioactive glass: From Hench to hybrids. *Act. Biomater.* **2013**, *9*, 4457–4486.
3. Owens, G.J.; Singh, R.K.; Foroutan, F.; Alquaysi, M.; Han, C.M.; Mahapatra, C.; Kim, H.W.; Knowles, J.C. Sol-gel based materials for biomedical applications. *Prog. Mater. Sci.* **2016**, *77*, 1–79.
4. Zheng, K.; Boccaccini, A.R. Sol-gel processing of bioactive glass nanoparticles: A review. *Adv. Coll. Interface Sci.* **2017**, *249*, 363–373.
5. Sharifianjazia, F.; Parvina, N.; Tahriri, M. Synthesis and characteristics of sol-gel bioactive $\text{SiO}_2\text{-P}_2\text{O}_5\text{-CaO-Ag}_2\text{O}$ glasses. *J. Non-Cryst. Solids* **2017**, *476*, 108–113.
6. Balamurugan, A.; Balamurugan, A.; Balossier, G.; Kannan, S.; Michel, J.; Rebelo, A.H.; Ferreira, J.M. Development and in vitro characterization of sol-gel derived $\text{CaO-P}_2\text{O}_5\text{-SiO}_2\text{-ZnO}$ bioglass. *Act. Biomater.* **2007**, *3*, 255–262.
7. Salman, S.; Salama, S.; Mosallam, H.A. The role of strontium and potassium on crystallization and bioactivity of $\text{Na}_2\text{O-CaO-P}_2\text{O}_5\text{-SiO}_2$ glasses. *Ceram. Int.* **2012**, *38*, 55–63.
8. Kheshen, A.E.; Khaliafa, F.A.; Saad, E.A.; Elwan, R.L. Effect of Al_2O_3 addition on bioactivity, thermal and mechanical properties of some bioactive glasses. *Ceram. Int.* **2008**, *34*, 1667–1673.
9. Errol, M.; Özyuguran, A.; Çelebican, O. Synthesis, Characterization, and In Vitro Bioactivity of Sol-Gel-Derived Zn, Mg, and Zn-Mg Co-Doped Bioactive Glasses. *Chem. Eng. Technol.* **2010**, *33*, 1066–1074.

10. Bari, A.; Bloise, N.; Fiorilli, S.; Novajra, G.; Vallet-Regí, M.; Bruni, G.; Torres-Pardo, A.; González-Calbet, J.M.; Visai, L.; Vitale-Brovarone, C. Copper-containing mesoporous bioactive glass nanoparticles as multifunctional agent for bone regeneration. *Act. Biomater.* **2017**, *55*, 493–504.
11. Baino, F.; Fiume, E.; Miola, M.; Leone, F.; Onida, B.; Verné, E. Fe-doped bioactive glass-derived scaffolds produced by sol-gel foaming. *Mater. Lett.* **2019**, *235*, 207–211.
12. Hadley, K.B.; Newman, S.M.; Hunt, J.R. Dietary zinc reduces osteoclast resorption activities and increases markers of osteoblast differentiation, matrix maturation, and mineralization in the long bones of growing rats. *J. Nutr. Biochem.* **2010**, *21*, 297–303.
13. Popp, J.R.; Love, B.J.; Goldstein, A.S. Effect of soluble zinc on differentiation of osteoprogenitor cells. *J. Biomed. Mater. Res. Part A* **2007**, *81*, 66–769.
14. E-Kady, A.E.; Ali, A.F. Fabrication and characterization of ZnO modified bioactive glass nanoparticles. *Ceram. Int.* **2012**, *38*, 1195–1204.
15. Bejarano, J.; Caviedes, P.; Palza, H. Sol-gel synthesis and in vitro bioactivity of copper and zinc-doped silicate bioactive glasses and glass-ceramics. *Biomed. Mater.* **2015**, *10*, 025001.
16. Hoa, B.T.; Hoa, H.T.T.; Tien, N.A.; Khang, N.H.D.; Guseva, E.V.; Tuan, N.A.; Vuong, B.X. Green synthesis of bioactive glass 70SiO₂-30CaO by hydrothermal method. *Mater. Lett.* **2020**, *274*, 128032.
17. Kokubo, T.; Takadama, H. How useful is SBF in predicting in vivo bone bioactivity. *Biomaterials* **2006**, *27*, 2907–2915.
18. Mosmann, T. Rapid colorimetric assay for cellular growth and survival: application to proliferation and cytotoxicity assays. *J. Immunol. Methods* **1983**, *65*, 55–63.
19. Xia, W.; Chang, J.J. Preparation and characterization of nano-bioactiveglasses (NBG) by a quick alkali-mediated (sol-gel) method. *Mater. Lett.* **2007**, *61*, 3251–3253.
20. Saravanapavan, P.; Hench, L.L. Mesoporous calcium silicate glasses. I. Synthesis. *J. Non-Cryst. Solids* **2003**, *318*, 1–13.
21. Román, J.; Padilla, S.; Vallet-Regí, M. Sol-gel glasses as precursors of bioactive glass ceramics. *Chem. Mater.* **2003**, *15*, 798–806.
22. Courthéoux, L.; Lao, J.; Nedelec, J.M.; Jallot, E. Controlled bioactivity in zinc-doped sol-gelderived binary bioactive glasses. *J. Phys. Chem. C* **2008**, *112*, 13663–13667.
23. Atkinson, I.; Anghel, E.M.; Predoana, L.; Mocioiu, O.C.; Jecu, L.; Raut, I.; Munteanu, C.; Culita, D.; Zaharescu, M. Influence of ZnO addition on the structural, in vitro behavior and antimicrobial activity of sol-gel derived CaO-P₂O₅-SiO₂ bioactive glasses. *Ceram. Int.* **2016**, *42*, 3033–3045.
24. Wu, C.; Chang, J. Mesoporous bioactive glasses: structure characteristics, drug/growth factor delivery and bone regeneration application. *Interface Focus* **2012**, *2*, 292–306.
25. Oudadesse, H.; Dietrich, E.; Gal, Y.L.; Pellen, P.; Bureau, B.; Mostafa, A.A.; Cathelineau, G. Apatite forming ability and cytocompatibility of pure and Zn-doped bioactive glasses. *Biomed. Mater.* **2011**, *6*, 1–9.

Publisher's Note: MDPI stays neutral with regard to jurisdictional claims in published maps and institutional affiliations.



© 2020 by the authors. Licensee MDPI, Basel, Switzerland. This article is an open access article distributed under the terms and conditions of the Creative Commons Attribution (CC BY) license (<http://creativecommons.org/licenses/by/4.0/>).